Analyst

RSC Publishing

PAPER

High sensitivity liquid phase measurements using broadband cavity enhanced absorption spectroscopy (BBCEAS) featuring a low cost webcam based prism spectrometer

Cite this: *Analyst*, 2013, **138**, 6372

Zhechao Qu,[a] Julia Engstrom,[a] Donald Wong,[a] Meez Islam[b] and Clemens F. Kaminski*[a]

Cavity enhanced techniques enable high sensitivity absorption measurements in the liquid phase but are typically more complex, and much more expensive, to perform than conventional absorption methods. The latter attributes have so far prevented a wide spread use of these methods in the analytical sciences. In this study we demonstrate a novel BBCEAS instrument that is sensitive, yet simple and economical to set up and operate. We use a prism spectrometer with a low cost webcam as the detector in conjunction with an optical cavity consisting of two $R = 0.99$ dielectric mirrors and a white light LED source for illumination. High sensitivity liquid phase measurements were made on samples contained in 1 cm quartz cuvettes placed at normal incidence to the light beam in the optical cavity. The cavity enhancement factor (CEF) with water as the solvent was determined directly by phase shift cavity ring down spectroscopy (PS-CRDS) and also by calibration with Rhodamine 6G solutions. Both methods yielded closely matching CEF values of ~60. The minimum detectable change in absorption (α_{min}) was determined to be 6.5×10^{-5} cm^{-1} at 527 nm and was limited only by the 8 bit resolution of the particular webcam detector used, thus offering scope for further improvement. The instrument was used to make representative measurements on dye solutions and in the determination of nitrite concentrations in a variation of the widely used Griess Assay. Limits of detection (LOD) were ~850 pM for Rhodamine 6G and 3.7 nM for nitrite, respectively. The sensitivity of the instrument compares favourably with previous cavity based liquid phase studies whilst being achieved at a small fraction of the cost hitherto reported, thus opening the door to widespread use in the community. Further means of improving sensitivity are discussed in the paper.

Received 29th July 2013
Accepted 5th September 2013

DOI: 10.1039/c3an01441j

www.rsc.org/analyst

Introduction

Absorption spectroscopy techniques are widely used in many fields, due to their relative simplicity, and ability to make easily quantifiable measurements requiring simple or no calibration protocols. However, since the signal loss is measured against a positive background the sensitivity is typically poor compared to zero background techniques, such as fluorescence. The sensitivity of an absorption measurement is directly proportional to the sample path length. Thus improvements can be made through use of multipass cells such as White's- or Herriot-cells in which the light path is folded several times through the sample chamber before detection,[1] but these approaches require cells with relatively large physical volumes and this can restrict applicability in the field, especially when dealing with analytes in the liquid phase.

In recent years cavity ring-down spectroscopy (CRDS)[2] and cavity enhanced absorption spectroscopy (CEAS)[3] have provided new means of increasing the path length. Here very long absorption path lengths can be achieved by placing the sample within a stable optical resonator and this improves sensitivity by many orders of magnitude over single pass absorption measurements. For both techniques the build-up of intra cavity power and cavity throughput depends on intra cavity losses, which include absorption by the sample. In CRDS, one typically injects light from a pulsed source into the cavity and measures the exponential decay rate of the light intensity exiting the cavity. CEAS is experimentally simpler to perform as here one couples light continuously into the optical cavity, and the wavelength is tuned over the absorption features of interest. As in conventional single pass absorption, one measures changes in the steady state transmission through the cavity in the absence and presence of absorbing species. A disadvantage of

[a]*Department of Chemical Engineering and Biotechnology, University of Cambridge, Pembroke Street, Cambridge CB2 3RA, UK. E-mail: cfk23@cam.ac.uk; Fax: +44 (0) 1223 334796; Tel: +44 (0)1223 (3)30133*

[b]*School of Science and Engineering, Teesside University, Borough Road, Middlesbrough, TS1 3BA, UK*

CEAS is that it requires a separate calibration to determine the baseline loss of the cavity,[4] whilst this is obtained directly in CRDS measurements.

The use of multiplexed CEAS measurements has been reported through use of broadband light sources such as arc lamps,[5,6] and light emitting diodes (LEDs).[7] Recently the use of incoherent, ultra wide bandwidth supercontinuum (SC) radiation has been demonstrated for use in CEAS both in the gas phase[8–11] and in the liquid phase.[12,13] Collectively these implementations of CEAS are referred to as broadband cavity enhanced absorption spectroscopy (BBCEAS). In BBCEAS the output from the cavity is spectrally dispersed and each wavelength component recorded in parallel. This permits entire absorption spectra to be captured in a single measurement,[14] dramatically reducing acquisition time relative to CEAS in which a spectrally narrow excitation line is scanned sequentially across the absorption features of interest.[15] BBCEAS requires use of a multiplex detector such as a photodiode array or a CCD.

LED light sources have excellent potential for use in BBCEAS offering low cost, high output stability, good power efficiency and long life times. They are furthermore available in most spectral windows from the near UV to the near infrared spectral regions. True broadband LEDs (>100 nm wavelength range) are restricted to white light LEDs, which typically emit between 400 and 750 nm. The successful coupling of LEDs with BBCEAS has allowed simple but sensitive measurements to be performed in both the gas and liquid phase.[16–19] To date the majority of cavity based studies have been performed on gas phase analytes as the background scattering and absorption in gases is comparatively small, and $>10^4$ passes are routinely achieved with high reflectivity mirrors and correspondingly long effective path length (10 s of km). Yet, the potential number of applications in the liquid phase is far greater than in the gas phase in chemical, biomedical, or process monitoring. However, in liquids the higher molecular density leads to increased scattering and solvents furthermore cause background absorption *via* overtone vibrations. These contribute to much higher background optical losses and limit the number of passes which can be achieved in liquids (typically <100). BBCEAS is in many ways ideal for liquid-phase measurements: liquid phase spectra have broader bandwidth (typically >50 nm) than corresponding gas phase spectra and they are also relatively unstructured. These attributes are ideally matched to the capability of BBCEAS. The experimental methodology is similar to conventional absorption spectroscopy, whilst the use of LED light sources enables the development of compact, economical, and power-efficient instruments. The total cost of LED-BBCEAS instruments is currently dominated by the cost of the dispersive spectrometer and detection system. Even simple spectrometers typically cost more than £1000, whereas the cost of the other major components are LED (~£5 for high intensity white LEDs), dielectric mirrors ($R = 0.99$, 400–700 nm, ~£200), 1 cm quartz cuvette (~£50), collimating and coupling optics and mounts (~£200).

The aim of this study is to demonstrate a reliable BBCEAS system for analysis of liquids based on a white LED and a prism based dispersive spectrometer with a webcam detector. The system is ideally matched to the requirements of liquid phase BBCEAS, simple to implement, and about 10 times lower in cost than comparable commercial solutions, opening the door to widespread implementation of high sensitivity liquid phase absorption spectroscopy in the field. We test the performance of the instrument *via* calibration using dye solutions containing Rhodamine 6G (Rh6G) and also demonstrate its application for sensitive measurements of nitrite concentrations using a BBCEAS variant of the Griess Assay. The Griess Assay is a well-established quantitative colourimetric method, commonly used to determine cellular NO concentrations in biological systems.[20] Recently it has found use as a means of measuring nitrite concentrations in marine and aquatic environments.[21] Increasing the sensitivity of such measurements is important in many fields and may lead to cost reductions by permitting lower reagent concentrations to be used at similar or better sensitivity than current methods.

The CEF value for the system, which is inversely related to the total per pass loss, is amongst the most useful figures of merit for liquid-phase measurements. Here CEF values were determined for the system by two independent methods, phase-shift CRDS (PS-CRDS) on the one hand, and measurements in known concentrations of Rh6G in solution on the other. Both results were in good agreement.

Experimental methodology

In CEAS systems, the transmitted light intensity is recorded rather than the cavity ring-down time. The absorption coefficient $\alpha(\lambda)$ of the sample at the limit of low loss and high mirror reflectivity can be calculated according to the following equation[22]

$$\alpha(\lambda) = 2.303\varepsilon C = \left[\frac{I_0(\lambda)}{I(\lambda)} - 1\right] \frac{1 - R_{\text{eff}}}{d} \quad (1)$$

where ε is the decadic molar extinction coefficient (M^{-1} cm^{-1}), C is the concentration (M), $I_0(\lambda)$ and $I(\lambda)$ are the intensities of the transmitted light in absence and presence of the absorber respectively, d is optical path length through the liquid sample, R_{eff} is the effective cavity reflectivity, and λ is the wavelength. Unlike CRDS measurements, CEAS is not a self-calibrating technique and the parameter R_{eff} must be determined through another measurement.

In this study we performed PS-CRDS for calibration.[23] In this method, continuous-wave, but intensity modulated, light is injected into the optical cavity. The phase shift φ between light entering and exiting the optical cavity is given by:

$$2\pi f\tau = -\tan\varphi \quad (2)$$

where f is the modulation frequency of the light source and τ is the photon ring-down time in the cavity, given by:

$$\tau = \frac{L}{c\left(1 - R_{\text{eff}} + \alpha(\lambda)d\right)} \quad (3)$$

We used an intensity modulated diode laser to calibrate the effective absorption path length in the liquid sample using the PS-CRDS technique. R_{eff} depends not only on the geometric

mean of the cavity mirror reflectivity but also on the scattering and absorbing losses of the cuvette, and the solvent related scattering and absorbing loss of the water present in the cuvette. The calibration can alternatively be obtained *via* the cavity enhancement factor (CEF) of the system.[13] Eqn (1) can be rearranged to show that the optical path length is enhanced by a factor of $(1 - R_{\text{eff}})^{-1}$compared to the single path absorption. Hence the CEF, which is a measure of the effective number of passes of light through the sample, can be written as:

$$\text{CEF} = \frac{1}{1 - R_{\text{eff}}} = \frac{\frac{I_0(\lambda)}{I(\lambda)} - 1}{2.303\varepsilon Cd} \quad (4)$$

The effective absorption length is $d_{\text{eff}} = \text{CEF} \times d$. The CEF is inversely related to the total optical loss, which is determined by the reflectivity of the cavity mirrors as well as by scattering and absorption characteristics of the cuvette and solvent placed inside the cavity. Clearly, the higher the reflectivity of the cavity mirrors the greater the effective length. However, increasing R_{eff} also reduces the amount of light transmitted through the cavity to the detector, thereby placing a limit on the highest reflectivity that can be used. In addition, if solvent and cuvette losses are much greater than mirror losses, increasing mirror reflectivity will only lead to marginal improvements of the CEF whilst greatly reducing the light intensity reaching the detector. As the signal to noise ratio on a spectrum is proportional to $\sqrt{I}$, with relatively low radiant flux light sources such as LEDs it is often found that the most sensitive results are obtained with mirrors featuring a relatively low reflectivity, and here we use $R = 0.99$ mirrors for that reason,[7] in stark contrast to gas phase measurements where $R = 0.99995$ mirrors are commonly used.[14]

The sensitivity of the detection system can be quantified using the minimum detectable change in absorption or noise equivalent absorption (α_{min}), which is the normalized standard deviation of the smallest detectable change in absorption (units of cm^{-1})[24] and is expressed as:

$$\alpha_{\text{min}} = \frac{\Delta I_{\text{min}}}{I}\left(\frac{1 - R_{\text{eff}}}{d}\right) \quad (5)$$

here ΔI_{min} is the minimum detectable change of the light intensity transmitted through the cavity.

Experimental setup

The experimental set-up for LED-BBCEAS is shown in Fig. 1, along with the modifications required for PS-CRDS calibration. A white LED (Luxeon Star, 1W) was used as the light source emitting between ~400 nm and 750 nm. The LED was mounted on a heat-sink to stabilise its spectral output, and required a 30 minutes warm up period. The output from the LED was directly coupled into a fibre (M35L01, Thorlabs) and passed through a collimating lens (LB1757, Thorlabs). This produced a parallel beam which was passed through a bandpass filter ($\lambda_{\text{max}} =$ 550 nm) and coupled into a 25 cm linear optical cavity formed by a pair of 1 inch diameter, plano-concave mirrors (Layertech, 0.5 m radius of curvature, nominal reflectivity $R = 0.99 \pm 0.5\%$ from 420 to 640 nm). The light exiting the cavity was focussed onto an output fibre optic cable (M37L01, Thorlabs) which was connected to the detection system.

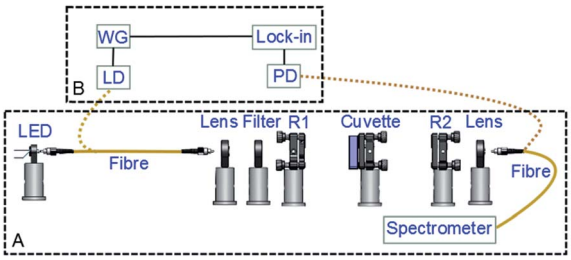

Fig. 1 Schematic setup of the LED based broadband cavity enhanced absorption spectrometer. R1, R2: cavity mirrors LD: laser diode, WG: waveform generator, PD: photo detector, lock-in: lock-in amplifier. Dotted lines show fibre connections for PS-CRDS calibration measurement: for this purpose light from the diode laser LD was injected into the cavity prior to the CEAS absorption experiments to determine the effective reflectivity of the cavity by PS-CRDS.

A 10 mm path length commercial quartz cuvette (Starna) was mounted on a 2D rotation optical stage to permit its rotational movement in the horizontal and vertical planes. The device was placed in the optical cavity at normal incidence to the propagation axis of light. The typical alignment procedure for the cavity and the cuvette was (1) the cavity was aligned without the cuvette, maximizing the light intensity of cavity output by iterative adjustment of the front and back cavity mirrors; (2) the cuvette was placed in the cavity with a reference solution of deionised water. This led to a decrease in the intensity of the cavity output due to optical losses of the cuvette windows and the solvent. The light intensity of the cavity output was optimised by finely adjusting the 2D rotation stage attached to the cuvette to ensure perpendicular alignment with respect to the light beam.

PS-CRDS calibration

For direct calibration of the effective cavity reflectivity R_{eff}, PS-CRDS was used. The output from a diode laser ($\lambda = 450$ nm, 120 mW, Nichia) was coupled into the input fibre (see beam path B in Fig. 1) and subsequently through the optical cavity containing a water filled cuvette. A waveform generator with a sinusoidal output waveform was used as the reference function driver for the diode laser. The light transmitted through the output fibre was detected using a photodiode detector (DET36A, Thorlabs). The phase shift of the transmitted signal with respect to the modulated waveform at the cavity input was measured with a lock-in amplifier (Stanford Research Systems SR830). The system response or zero phase angle φ_0 was acquired by removing one of the cavity mirrors. To maximise the measured phase shift, the modulation frequency should be chosen such that $2\pi\tau f \approx 1$,[25] and as ring-down times were on the microsecond timescale, consequently this led to the choice of a 2 MHz modulation frequency. This gave a phase shift of around 45°. CRDS was not the only method used to determine the R_{eff}. An alternative method of determining R_{eff} through the measurement of the CEF by using a dye with a well-known absorption,[7,13] was also performed as a comparison.

The effective cavity reflectivity R_{eff} was first measured using PS-CRDS. The measured phase shifts and corresponding reflectivity values were -38.6^0 and 98.64% at 450 nm for a cavity containing a cuvette filled with deionised water. Then using the manufacturers published data on the spectral response of the mirrors, the calibration was extended to the required wavelength range. The effective cavity reflectivity R_{eff} at 527 nm (λ_{max} for Rh6G) was 98.34%, corresponding to a CEF value of ~60 and hence an effective optical path length of 60 cm for the 1 cm cuvette used.

Webcam based prism spectrometer

The spectrum of the light transmitted through the cavity was recorded using a prism spectrometer equipped with a webcam detector (C200, Logitech, 640 × 480 pixels, 8 bit A/D convertor, ~£10), shown in Fig. 2.This greatly reduced the overall cost of system. Before use, the webcam case was opened, and the lens and filter assembly were removed leaving just the CCD detector. The light exiting the output fibre was collimated onto the prism (47-275, Edmund Optics, ~£60) dispersed, and then focused on the webcam CCD. The total cost of the spectrometer components was ~£70, whilst the overall cost of the BBCEAS instrument was ~£500. The webcam was interfaced *via* USB to a computer and data was acquired using a custom LabVIEW program. The horizontal pixel position needed to be calibrated to produce a wavelength scale. This was done using a green LED peaking at 525 nm and Helium–Neon (HeNe) lasers at 543 and 594 nm. In order to verify the accuracy and sensitivity of the custom built webcam spectrometer for BBCEAS measurements, a commercial spectrometer (USB4000, Ocean Optics) was also used to make measurements. The webcam CCD was a colour model with red, green and blue (RGB) channels. In all measurements reported, the output over all RGB channels was averaged to produce an intensity value.

Scientific grade CCD cameras show a highly linear response with input intensity. This is not the case in consumer grade cameras, where the input response is set to mimic that of the human eye. Fig. 3 shows the intensity response of the webcam CCD used in the present work (red stars). As can be seen in Fig. 3, the signal is nonlinear with input light intensity due to a gamma correction[26] applied on board by the webcam control circuitry. This is a commonly used technique to maximise the amount of tonal information in a picture, such that more of the intensity scale is used for darker tones than for the brighter tones. It was not possible to remove the gamma correction step directly, instead we used a 3rd order polynomial function to linearise the response of the CCD (solid red line in Fig. 3) and this correction was subsequently used in all measurements reported.

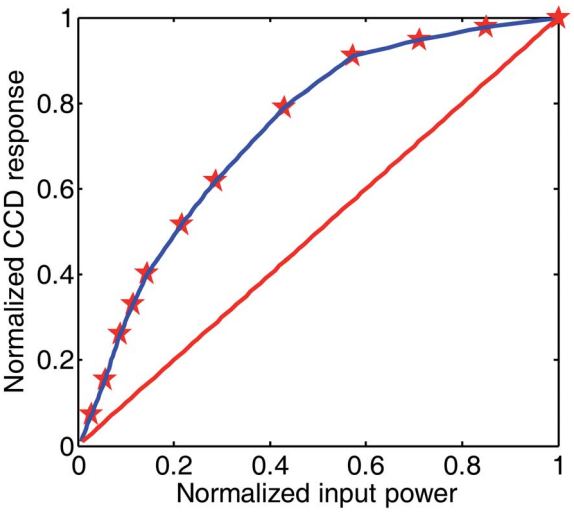

Fig. 3 Normalized CCD response *versus* input power for the webcam CCD used in experiments presented. Red stars: measured data, blue line: fitted curve, red line: calibrated and hence linearised response curve.

The dynamic range of a CCD sensor is a combination of digital dynamic range (bit depth) and the optical dynamic range.[27] The latter is typically specified as the maximum achievable signal divided by the CCD noise, where the signal strength is determined by the full-well capacity of the pixels, and the noise is the sum of dark and read-out noise contributions. As the dynamic range of a CCD is increased, the ability to quantitatively measure the dimmest intensities in an image is improved. The bit depth refers to the binary range of possible grayscale values utilized by the A/D converter to translate analogue image information into discrete digital values. It determines the size of the grayscale increments, with higher bit depths corresponding to a greater range of useful image information available from the camera. For instance, the webcam CCD which has an 8-bit (256 grayscale levels, between 0 and 255) A/D converter might be used to sample data at 1 part in 256. In the experiments, to use the full dynamic range of the webcam CCD, the input light intensity of the CCD should be near the saturating value I_{sat}, which means the grayscale value of the CCD is approximately 255. The minimum detectable change of the light intensity is I_{sat} divided by 256. It should be clear that optical dynamic range and bit depth are two different characteristics of the camera. It needs a high dynamic range to capture faint signal without blowing out the highlights, and to capture fine gradations of intensity in the image. However, it also needs a high bit depth to actually render all of those captured steps into a useable digital output. The relative error of the LED light intensity is measured by the webcam CCD camera as shown in Fig. 4, the value of $\Delta I/I$ is smaller than 0.2% in the

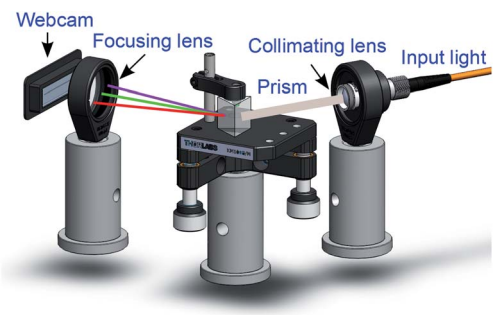

Fig. 2 Schematic diagram of the webcam spectrometer.

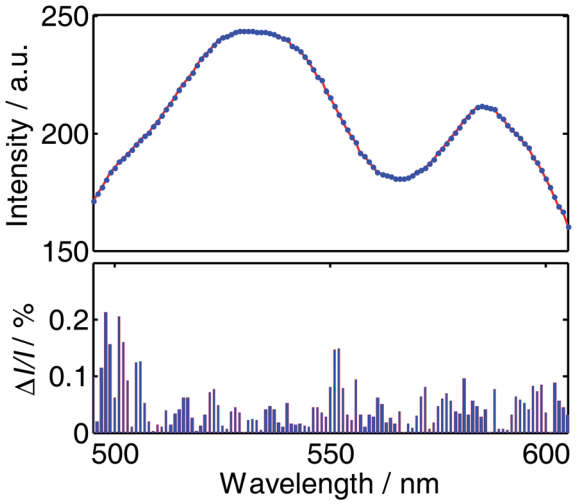

Fig. 4 The upper plot is the spectrum of the cavity output between 500 and 600 nm as measured by the webcam CCD, the lower plot is the corresponding relative error of the light intensity, Δ*I*/*I*.

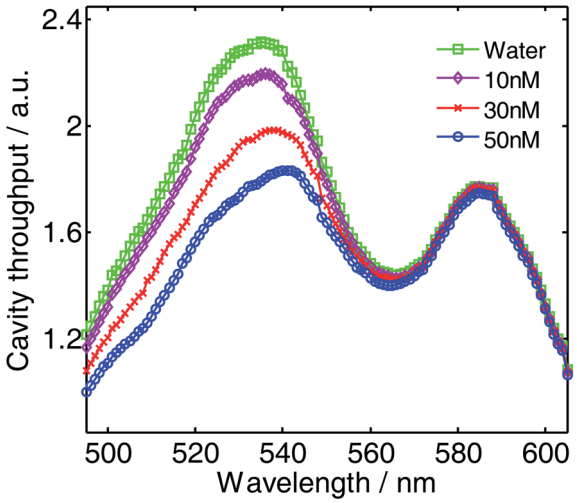

Fig. 5 The spectra of cavity throughput corresponding to the cuvette filled with pure water, 10 nM, 30 nM, and 50 nM Rh6G solutions.

range 500 to 600 nm, ΔI is the standard deviation of 20 repeated measurements with the webcam. When using an 8-bit A/D converter, the minimum detectable intensity change is 0.39% (=1/256) which is larger than the measured result 0.2%. It is clear that the webcam CCD camera has a high optical dynamic range but low bit depth, in this case we are not taking full advantage of all of those fine gradations of intensity that the CCD camera has captured.

Results and discussion

Rh6G, *N*-(1-naphthyl) ethylenediamine dihydrochloride, sulfanilic acid, phosphoric acid, and sodium nitrite used in this work were purchased from Sigma (Sigma, UK). All solutions were made up using deionized water (18.2 MΩ cm^{-1}). A dilution series of Rh6G solutions in the concentration range from 5 nM to 100 nM were prepared. Solutions were introduced into the cuvette using a 20 ml plastic syringe. For each absorption measurement, the cuvette was initially flushed with deionised water, and the output spectrum of the cavity over the wavelength range from 500–600 nm was recorded, averaged over 20 traces.

The light transmitted through the cavity, as shown in Fig. 5, is spectrally dispersed using a prism and then detected by the webcam CCD. The average of 20 frames corresponding to a total acquisition of 1 second is shown.

Fig. 6 shows absorption spectra of Rh6G (peak absorption near 527 nm) in deionized water at 10, 20, 30, and 50 nM concentrations. The plot also displays the water (solvent) baseline. In most BBCEAS applications, the noise on this baseline allows the sensitivity of the measurement to be calculated,[6] *via* the minimum detectable change in absorption α_{min} from the 1σ noise on the baseline (σ is the standard deviation of the baseline). Using this baseline, α_{min} is approximately 1.1×10^{-5} cm^{-1}. This means that the minimum detectable change of the light intensity should be 1×10^{-4} which is smaller than what is resolvable (0.4%) by the 8-bit A/D converter of the

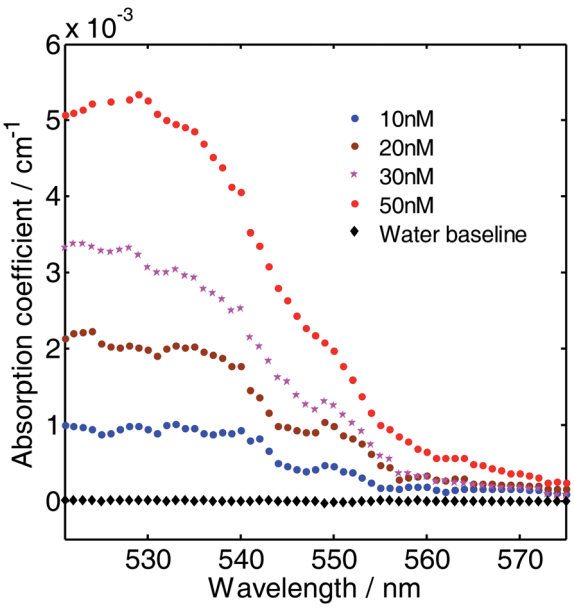

Fig. 6 Absorption spectra of Rh6G in deionized water at 10, 20, 30, and 50 nM concentrations. The spectra were acquired using the webcam CCD camera (50 ms single-shot exposure time). Averages of 20 single shot spectra are shown here corresponding to 1s total acquisition time.

webcam CCD. Hence it is not possible to calculate α_{min} using the baseline absorption method. Instead, from eqn (5), α_{min} is limited to 6.5×10^{-5} cm^{-1} at 527 nm for a signal acquisition time of 1 s on the webcam CCD.

The Rh6G measurements were made with both the prism spectrometer and a commercial Ocean Optics spectrometer over a range of concentrations from 10 nM to 100 nM. A linear dependence of the absorption on sample concentration was obtained in both cases. Fig. 7 shows the absorption at 527 nm *versus* concentration for Rh6G and the corresponding error-weighted linear fits to the measurements. The equation of the linear fit to the Ocean Optics spectrometer data was $y = 0.0057x + 0.0085$ with

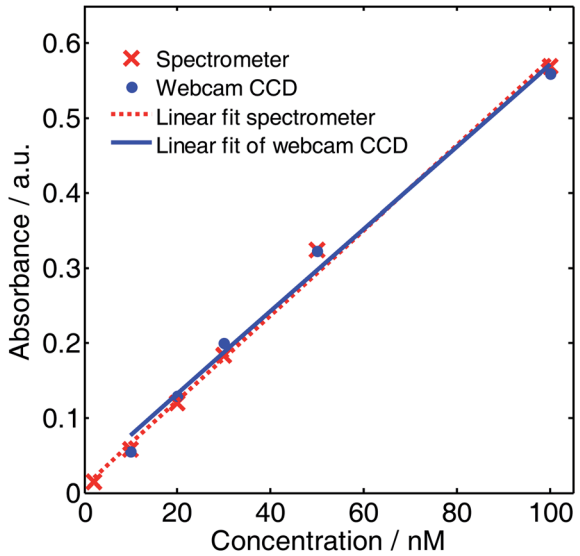

Fig. 7 The absorption *versus* concentration plot of Rh6G, in the range 5 nM to 100 nM. Red line: linear fit of the results measured by the commercial Ocean Optics spectrometer, blue line: linear fit of the results measured by the webcam spectrometer.

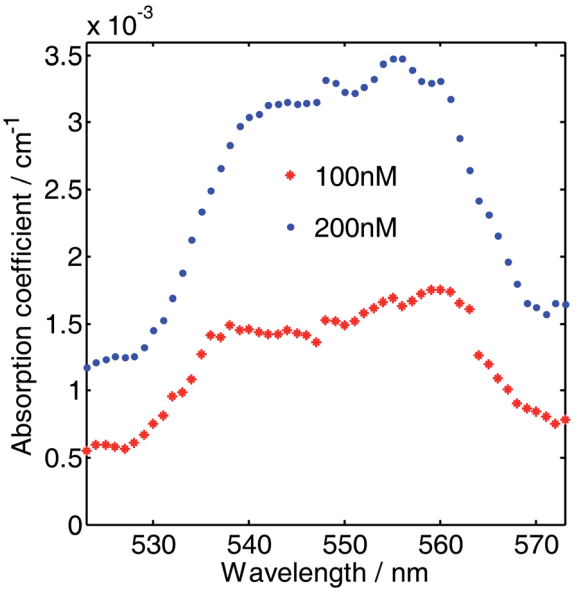

Fig. 8 The absorption spectra of the Griess reagent mixed with 100 nM and 200 nM concentrations of nitrite solution.

$R^2 = 0.9967$. The CEF can be obtained from the slope of the linear fit, CEF $\approx$ 61. Similarly, the equation of the linear fit to the webcam spectrometer data was $y = 0.0055x + 0.022$ with $R^2 = 0.9958$ and the CEF was 59. Thus the CEF value measured by using the dye calibration method for both spectrometers is in good agreement with that measured by PS-CRDS. The LOD for Rh6G can be calculated from the α_{min} value[7] (eqn (5)), and yields a value of ~850 pM using the webcam spectrometer.

The Griess Assay is a commonly used quantitative colourimetric test for the determination of aqueous phase nitrite (NO_2^-) concentration.[28] It relies on the formation of an Azo dye by the reaction of sulfanilamide hydrochloride and *N*-(1-naphthyl) ethylenediamine dihydrochloride with nitrite. The optical absorption of this Azo dye (formed in the presence of nitrite) is centred at ~550 nm and is linearly proportional to the concentration of nitrite. The Griess Assay has been successfully used to measure nitrite concentration in a range of sample environments, including: raw seawater, snow, and tap water.[29] It can also be used to quantify the amount of nitric oxide (NO), an important mediator in many biological processes,[30,31] as nitrite is the stable oxidation product of NO.

To prepare the Griess reagent, component A [*N*-(1-naphthyl) ethylenediamine dihydrochloride 0.1% (1 mg mL^{-1}) solution] and component B [sulfanilic acid 1% (10 mg mL^{-1})] were first prepared in 5% phosphoric acid solutions, respectively, and then mixed together in equal volumes of A and B to form the Griess reagent. Nitrite standard solutions in the concentration range from 10 nM to 1 μM were prepared by dissolving sodium nitrite in deionized water. To perform a nitrite determination measurement, the Griess reagent and nitrite solution were mixed in a beaker and left to stand for at least 20 minutes to ensure that the Griess reaction had reached completion before the Azo dye absorption spectrum was measured. Rather than using deionised water to determine the background for our spectral measurements, a 1 : 1 mixture of deionised water and the Griess reagent was employed. Fig. 8 shows plots of the absorption coefficient recorded in the wavelength range 520 to 570 nm for the Griess reagent mixed with 100 nM and 200 nM concentrations of nitrite solutions. For each measurement, the absorption spectrum of the 1 : 1 mixture of Griess reagent and deionised water was acquired, and then a 1 : 1 mixture of Griess reagent and the nitrite solution of interest. From calculating the minimum detectable absorption coefficient, the estimated limit of detection (LOD) for nitrite solution is 3.7 nM.

Table 1, compares the sensitivity of the webcam BBCEAS set-up with selected previous liquid phase cavity enhanced absorption measurements. These have employed different cavity techniques with considerable differences in light sources, base path length, mirror reflectivity used, sensitivity obtained and also estimated overall cost. The sensitivity obtained in this study is comparable to those achieved by other cavity studies utilising similar base path length but is significantly less costly to implement than all previous methods, some of which are more than two orders of magnitude more expensive. A closer comparison was made with a previous study by Islam *et al.*[7] which used a similar methodology and experimental setup. The sensitivities are similar although Islam *et al.* used a 5 times shorter base path length whilst the use of a webcam based prism spectrometer in this study has allowed a ~5 fold reduction in the cost of the experimental setup. The recent CRDS study of Rushworth *et al.*[21] has also made measurements using the Griess Assay. The reported LOD of 1.4 nM is similar to that from this study. Whilst a shorter base path length has been used, higher reflectivity mirrors were also used and so the overall sensitivities of the two techniques is broadly similar but the cost of the current setup is ~20 fold less costly to implement.

Table 1 Sensitivity comparison of the BBCEAS webcam-based set-up in this work to previous cavity enhanced absorption measurements[a]

Study	Light source	Method	R	L_{abs}/cm	α_{min}/cm^{-1}	Cost
This work	LED	BBCEAS	0.99	1	6.5×10^{-5}	~£0.5k
Islam *et al.*[7]	LED	BBCEAS	0.99	0.2	5.1×10^{-5}	>£3k
Seetohul *et al.*[19]	LED	BBCEAS	0.999	20	2.8×10^{-7}	>£3k
Fiedler *et al.*[32]	Xe arc lamp	CEAS	0.99	1	2×10^{-5}	>£10k
Bahnev *et al.*[33]	YAG laser	CRDS	0.9998	0.2	1.6×10^{-4}	>£50k
Snyder *et al.*[34]	YAG laser	CRDS	0.9993	0.03	2.5×10^{-4}	>£30k
van der Sneppen *et al.*[35]	OPO laser	CRDS	0.99996	0.2	1.0×10^{-5}	>£100k
Kiwanuka *et al.*[12]	SC laser	BBCEAS	0.99	5.4	9.1×10^{-7}	>£30k
Rushworth *et al.*[21]	YAG laser	CRDS	0.998	0.2	2.9×10^{-5}	>£10k

[a] The table shows the cavity enhanced method used: reflectivity of cavity mirror R, single pass sample absorption length L_{abs}, minimum detectable change in absorption α_{min}.

The current sensitivity of the setup is limited by the performance of the 8-bit A/D converter on the webcam. A webcam or CCD sensor with a ≥12 bit A/D converter would overcome this limit and lead to a potential 6 fold improvement in sensitivity for 1 s signal acquisition. Relatively low cost cameras (~£300) of this type are available[36] and although considerably more expensive than a webcam would only increase the overall cost of the experimental setup moderately (to a total cost of~£800), to be still significantly lower than for all other existing setups. The path length of the cuvette is 1 cm, and so using a cuvette with longer path length would be a simple way of further increasing the sensitivity. Higher reflectivity $R > 0.995$ mirrors could also be used to increase the CEF and thus effective path length but these would need to be coupled with higher intensity LEDs to avoid a reduction in intensity at the detector.

Conclusion

A BBCEAS setup employing a novel low cost prism spectrometer with a simple webcam detector has been implemented with a white LED source and two $R = 0.99$ cavity mirrors to make liquid-phase measurements on solutions of Rh6G dye and also nitrite using the Griess Assay. The effective measurement path length was determined directly using PS-CRDS and also by calibration using Rh6G dye solutions. Both methods yielded consistent CEF values of ~60. The measured sensitivity of 6.5×10^{-5} cm^{-1} was comparable to similar previous liquid phase cavity studies but achievable at a cost that was between ~5 and 200 fold lower. The sensitivity of the present instrument can be greatly improved by using a CCD with ≥12 bit A/D convertor resolution.

References

1 R. F. Curl, F. Capasso, C. Gmachl, A. A. Kosterev, B. McManus, R. Lewicki and F. K. Tittel, Quantum cascade lasers in chemical physics, *Chem. Phys. Lett.*, 2010, **487**, 1–18.

2 S. Xu, G. Sha and J. Xie, Cavity ring-down spectroscopy in the liquid phase, *Rev. Sci. Instrum.*, 2002, **73**, 255–258.

3 R. Symes, R. Sayer and J. Reid, Cavity enhanced droplet spectroscopy: principles, perspectives and prospects, *Phys. Chem. Chem. Phys.*, 2004, **6**, 474–487.

4 T. Laurila, I. S. Burns, J. Hult, J. H. Miller and C. F. Kaminski, A calibration method for broad-bandwidth cavity enhanced absorption spectroscopy performed with supercontinuum radiation, *Appl. Phys. B: Lasers Opt.*, 2010, **102**, 271–278.

5 M. Islam, L. Ciaffoni, G. Hancock and G. A. D. Ritchie, Demonstration of a novel laser-driven light source for broadband spectroscopy between 170 nm and 2.1 μm, *Analyst*, 2013, **138**, 4741–4745.

6 S. B. Darby, P. D. Smith and D. S. Venables, Cavity-enhanced absorption using an atomic line source: application to deep-UV measurements, *Analyst*, 2012, **137**, 2318–2321.

7 M. Islam, L. N. Seetohul and Z. Ali, Liquid-phase broadband cavity-enhanced absorption spectroscopy measurements in a 2 mm cuvette, *Appl. Spectrosc.*, 2007, **61**, 649–658.

8 W. Denzer, G. Hancock, M. Islam, C. E. Langley, R. Peverall, G. A. D. Ritchie and D. Taylor, Trace species detection in the near infrared using Fourier transform broadband cavity enhanced absorption spectroscopy: initial studies on potential breath analytes, *Analyst*, 2011, **136**, 801–806.

9 C. F. Kaminski, R. S. Watt, A. D. Elder, J. H. Frank and J. Hult, Supercontinuum radiation for applications in chemical sensing and microscopy, *Appl. Phys. B: Lasers Opt.*, 2008, **92**, 367–378.

10 J. M. Langridge, T. Laurila, R. S. Watt, R. L. Jones, C. F. Kaminski and J. Hult, Cavity enhanced absorption spectroscopy of multiple trace gas species using a supercontinuum radiation source, *Opt. Express*, 2008, **16**, 10178–10188.

11 R. S. Watt, T. Laurila, C. F. Kaminski and J. Hult, Cavity Enhanced Spectroscopy of High-Temperature H_2O in the Near-Infrared Using a Supercontinuum Light Source, *Appl. Spectrosc.*, 2009, **63**, 1389–1395.

12 S. S. Kiwanuka, T. Laurila and C. F. Kaminski, Sensitive method for the kinetic measurement of trace species in liquids using cavity enhanced absorption spectroscopy with broad bandwidth supercontinuum radiation, *Anal. Chem.*, 2010, **82**, 7498–7501.

13 L. van der Sneppen, G. Hancock, C. Kaminski, T. Laurila, S. R. Mackenzie, S. R. Neil and P. R. Unwin, Following interfacial kinetics in real time using broadband evanescent wave cavity-enhanced absorption spectroscopy:

a comparison of light-emitting diodes and supercontinuum sources, *Analyst*, 2010, **135**, 133–139.
14 M. Schnippering, *et al.* Evanescent wave broadband cavity enhanced absorption spectroscopy using supercontinuum radiation: a new probe of electrochemical processes, *Electrochem. Commun.*, 2008, **10**, 1827–1830.
15 M. Gupta, Highly-precise measurements of ambient oxygen using near-infrared cavity-enhanced laser absorption spectrometry, *Anal. Chem.*, 2012, **84**, 7987–7991.
16 T. F. Kahan, R. a. Washenfelder, V. Vaida and S. S. Brown, Cavity-enhanced measurements of hydrogen peroxide absorption cross sections from 353 to 410 nm, *J. Phys. Chem. A*, 2012, **116**, 5941–5947.
17 M. Triki, P. Cermak, G. Méjean and D. Romanini, Cavity-enhanced absorption spectroscopy with a red LED source for NOx trace analysis, *Appl. Phys. B: Lasers Opt.*, 2008, **91**, 195–201.
18 L. N. Seetohul, Z. Ali and M. Islam, Broadband cavity enhanced absorption spectroscopy as a detector for HPLC, *Anal. Chem.*, 2009, **81**, 4106–4112.
19 L. N. Seetohul, Z. Ali and M. Islam, Liquid-phase broadband cavity enhanced absorption spectroscopy (BBCEAS) studies in a 20 cm cell, *Analyst*, 2009, **134**, 1887–1895.
20 J. Dutt and J. Davis, Current strategies in nitrite detection and their application to field analysis, *J. Environ. Monit.*, 2002, **4**, 465–471.
21 C. M. Rushworth, Y. Yogarajah, Y. Zhao, H. Morgan and C. Vallance, Sensitive analysis of trace water analytes using colourimetric cavity ringdown spectroscopy, *Anal. Methods*, 2013, **5**, 239–247.
22 S. M. Ball, J. M. Langridge and R. L. Jones, Broadband cavity enhanced absorption spectroscopy using light emitting diodes, *Chem. Phys. Lett.*, 2004, **398**, 68–74.
23 R. Engeln, G. Helden, G. von Berden and G. Meijer, Phase shift cavity ring down absorption spectroscopy, *Chem. Phys. Lett.*, 1996, **262**, 105–109.
24 C. M. Rushworth, *et al.* Cavity-enhanced optical methods for online microfluidic analysis, *Chem. Phys. Lett.*, 2012, **554**, 1–14.
25 B. Ouyang and R. L. Jones, Understanding the sensitivity of cavity-enhanced absorption spectroscopy: pathlength enhancement *versus* noise suppression, *Appl. Phys. B: Lasers Opt.*, 2012, **109**, 581–591.
26 G. J. Klinker, S. A. Shafer and T. Kanade, A physical approach to color image understanding, *International Journal of Computer Vision*, 1990, **4**, 7–38.
27 K. Spring, Scientific imaging with digital cameras, *BioTechniques*, 2000, **29**, 70–76.
28 P. Griess, Bemerkungenzu der Abhandlung der HH.Weselsky und Benedikt Uebereinige Azoverbindungen, *Ber. Dtsch. Chem. Ges.*, 1879, **12**, 426–428.
29 M. D. Patey, M. J. Rijkenberg, P. J. Statham, M. C. Stinchcombe, E. P. Achterberg and M. Mowlem, Determination of nitrate and phosphate in seawater at nanomolar concentrations, *TrAC, Trends Anal. Chem.*, 2008, **27**, 169–182.
30 S. Archer, Measurement of nitric oxide in biological models, *FASEB J.*, 1993, **7**, 349–360.
31 W. Tracey, J. Linden, M. Peach and R. Johns, Comparison of spectrophotometric and biological assays for nitric oxide (NO) and endothelium-derived relaxing factor (EDRF): nonspecificity of the diazotization reaction for NO and failure to detect EDRF, *J. Pharmacol. Exp. Ther.*, 1990, **252**, 922–928.
32 S. Fiedler, A. Hese and A. Ruth, Incoherent broad-band cavity-enhanced absorption spectroscopy of liquids, *Rev. Sci. Instrum.*, 2005, **76**, 023107.
33 B. Bahnev, *et al.* Miniaturized cavity ring-down detection in a liquid flow cell, *Anal. Chem.*, 2005, **77**, 1188–1191.
34 K. L. Snyder and R. N. Zare, Cavity ring-down spectroscopy as a detector for liquid chromatography, *Anal. Chem.*, 2003, **75**, 3086–3091.
35 L. van der Sneppen and A. Wiskerke, Cavity ring-down spectroscopy for detection in liquid chromatography: extension to tunable sources and ultraviolet wavelengths, *Appl. Spectrosc.*, 2006, **60**, 931–935.
36 http://www.modernastronomy.com/camerasGuider.html.